

Synthesis and Structural Properties of Adamantane-Substituted Amines and Amides Containing an Additional Adamantane, Azaadamantane or Diamantane Moiety

Maxime Bonsir,^{*,[a]} Alan R. Kennedy,^[b] and Yves Geerts^{*,[a, c]}

Introduction of adamantane moieties on diamondoids such as adamantane, 2-azaadamantane or diamantane by amide formation and reduction to the corresponding amine was performed in a straightforward and easy way by amidation under Schotten–Baumann conditions and reduction with $\text{BH}_3 \cdot \text{THF}$. The obtained amides and amines were studied in terms of structural properties towards the perspective of

transformation into nanodiamonds. Crystal structure and dynamic NMR experiments of the most crowded amide obtained gave structural insights into the effect of bulkiness and steric strain on out-of-planarity of amide bonds (16.0°) and the kinetics and thermodynamics of amide bond rotation ($\Delta G_{298\text{K}}^\ddagger = 11.5\text{--}13.3 \text{ kcal} \cdot \text{mol}^{-1}$).

Introduction

Adamantane 1 is a tricyclic cage compound of $\text{C}_{10}\text{H}_{16}$ formula. The incorporation of adamantane fragments in pharmaceuticals has an effect of improving the lipophilicity and stability of drugs.^[1,2] Examples of nitrogen-containing pharmaceuticals derived from adamantane are numerous and usually exhibit antiviral, anti-Parkinsonian or anti-Alzheimer properties.^[1,2] Structurally simple examples are amantadine 2, rimantadine 3 or memantine 4. (Figure 1) Another feature of adamantane is its superimposability to the diamond lattice: it is, in fact, the smallest molecular representative of the diamond family. Accordingly, adamantane is a member of a class of molecules called diamondoids, which are molecules possessing at least one adamantane unit which are totally or largely superimposable on the diamond lattice. Heteroatom-substituted diamondoids also exist, with 2-azaadamantane 5 (Figure 1) being a prime example. Other typical members of the diamondoid

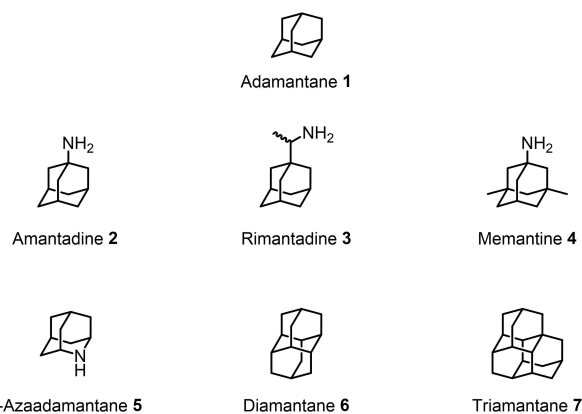


Figure 1. Structure of pharmaceuticals derived from adamantane and of diamondoids.

family are face-fused polymantanes, often referred to as “higher-order diamondoids”, with examples such as diamantane 6 or triamantane 7 which are formed of two and three face-fused adamantane units respectively (Figure 1). These structural motifs are comparatively less used in drug design and still need to prove their worth as useful pharmacophore add-ons.^[1]

There is a growing interest in materials chemistry in the use of diamondoids for diamond formation, which is an area of research that we are focused on. In recent years, it has been shown that diamondoids such as adamantane,^[3–7] (poly)haloadamantanes,^[8–10] azaadamantanes,^[11] adamantane carbonitrile^[7] or pentamantane^[12] can be used as precursors or seeds of nanodiamonds under high-pressure high-temperature conditions (HPHT synthesis) and for chemical vapor deposition methods (CVD synthesis). The presence of color centers in (nano)diamonds is responsible for their fluorescence properties, which are exploited for biomedical applications and quantum technologies such as nanoscale magnetometry, in-cell thermometry, spin cartography and qubit engineering.^[13–17] The typical example of a color center in nanodiamonds is the

[a] M. Bonsir, Prof. Dr. Y. Geerts
Laboratoire de Chimie des Polymères, Faculté des Sciences
Université Libre de Bruxelles (ULB)
Boulevard du Triomphe, CP 206/01, 1050 Bruxelles (Belgium)
E-mail: maxime.bonsir@ulb.be
yves.geerts@ulb.be

[b] Dr. A. R. Kennedy
Department of Pure and Applied Chemistry
University of Strathclyde
295 Cathedral Street
G1 1XL Glasgow (Scotland, UK)

[c] Prof. Dr. Y. Geerts
International Solvay Institutes for Physics and Chemistry
Université Libre de Bruxelles (ULB)
Boulevard du Triomphe, CP 231, 1050 Bruxelles (Belgium)

Supporting information for this article is available on the WWW under <https://doi.org/10.1002/open.202200031>

© 2022 The Authors. Published by Wiley-VCH GmbH. This is an open access article under the terms of the Creative Commons Attribution Non-Commercial NoDerivs License, which permits use and distribution in any medium, provided the original work is properly cited, the use is non-commercial and no modifications or adaptations are made.

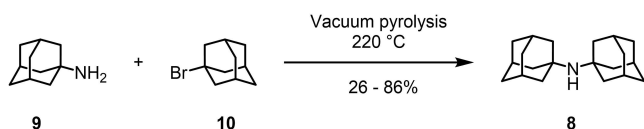
nitrogen-vacancy center, which is formed by the replacement of two neighboring carbon atoms by a nitrogen atom next to a vacancy site. This leads to the question of whether nitrogen-containing diamondoids can be used as efficient precursors or seeds of fluorescent nanodiamonds by a bottom-up approach. Current results indicate that this might indeed be the case.^[7,11] Furthermore, we hypothesize that an increase in the content of diamondoid fragments in a molecule will lead to a more efficient synthesis of nanodiamonds. We were therefore interested in the synthesis of amines and amides bearing multiple diamondoid fragments and studying their structural properties by X-ray diffraction studies, dynamic NMR experiments and thermal analyses in order to assess their potential suitability for nanodiamond formation. In particular, we were interested in studying the influence of adamantane, diamantane and azaadamantane fragments.

Amination and amidation of adamantane and other diamondoids has largely been motivated by their pharmacological applications and various well-established procedures can be followed to obtain such structures.^[1,2,18,19] Since the develop-

ment of these protocols was mostly fueled by pharmacological interest, there has been a low impulse for the N-linking of multiple diamondoid fragments due to the excessive lipophilicity that would arise from such molecules. The synthetic challenge in N-linking two diamondoid fragments is undoubtedly the steric hindrance, since each fragment is considerably sterically hindered. This can be observed with the requirement of harsh conditions for the synthesis of *N,N*-di-1-adamantylamine **8** from 1-adamantylamine **9** and 1-bromoadamantane **10** with variable yields (Scheme 1).^[20–26]

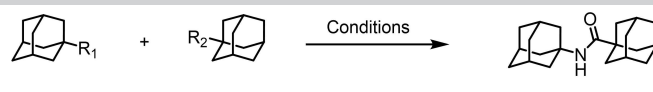
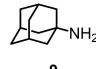
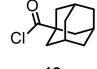
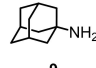
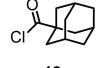
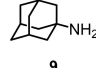
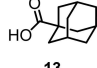
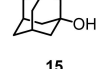
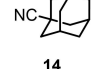
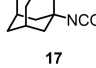
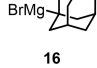
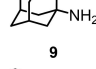
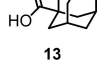
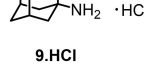
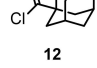
A few other examples reporting the syntheses of amides bearing two adamantane fragments are known.^[27] The amide with the most occurrences in the literature is 1-(*N*-(1-adamantyl))adamantanecarboxamide **11a** which is made of two adamantane fragments linked by an amide bond at bridgehead positions. Summarized reaction conditions are presented in Table 1 and in the following paragraph.

In 1996, Dubowchik et al. reported the synthesis of **11a** by coupling the corresponding carbonyl chloride **12** and amine **9** in the presence of pyridine, obtaining a yield of 89%.^[21] The following reduction with the borane-THF complex provided the corresponding amine **11b** with a yield of 91%. In 1998, Rudkevich et al. synthesized **11a** under Schotten–Baumann conditions by coupling amine **9** with carbonyl chloride **12** in a biphasic EtOAc/H₂O system in the presence of K₂CO₃ with a yield of 80–90%.^[28] In 2007, Kas'yan et al. synthesized **11a** in 55% yield by acylation of the corresponding amine **9** and carboxylic acid **13** in the presence of triethylamine. Other



Scheme 1. Synthesis of **8** by pyrolysis of the corresponding amine and bromide.

Table 1. Reported synthetic conditions for the synthesis of **11a**.

					
Ad-R ₁ fragment	Ad-R ₂ fragment	Conditions	Yield [%]	Reference	
 9	 12	Pyridine, CH ₂ Cl ₂ , r. t.	89	[21]	
 9	 12	K ₂ CO ₃ , EtOAc/H ₂ O (1:1), r. t.	80–90	[28]	
 9	 13	Et ₃ N, CHCl ₃ , r. t.	55	[27]	
 15	 14	[BMIM(SO ₃ H)][OTf], ^[a] AcOH, 80 °C	76	[29]	
 17	 16	Et ₂ O, 0 °C to r. t.	75	[30]	
 9	 13	BTFHH, DIPEA, ^[b] CH ₂ Cl ₂ , r. t. to 80 °C	78	[31]	
 9.HCl	 12	DIPEA, CH ₂ Cl ₂ , r. t.	87	[32]	

[a] BMIM = 1-butyl-3-methylimidazolium; [b] BTFHH = bis(tetramethylene)fluoroformamidinium hexafluorophosphate, DIPEA = *N,N*-diisopropylethylamine.

adamantane-derived amides were synthesized using the same method in moderate to good yields.^[27] Notably, these authors also showed that when the amide carbonyl group is located next to the adamantane fragment (as is the case for **11a**), reduction with LiAlH_4 was inhibited, even at increased reaction temperatures. Only when the carbonyl group was located further away from the adamantane fragment (a CH_2 spacer being long enough) was the reduction with LiAlH_4 successful. In 2011, Kalkhambkar et al. synthesized **11a** by using Brønsted-acidic imidazolium ionic liquid $[\text{BMIM}(\text{SO}_3\text{H})][\text{OTf}]$ as catalyst ($\text{BMIM} = 1\text{-butyl-3-methylimidazolium}$), using the corresponding nitrile **14** and the alcohol derivative **15** and arriving at a yield of 76%.^[29] Schäfer et al. have shown, in 2012, that **11a** can be synthesized in 75% yield by coupling the corresponding Grignard reagent **16** and isocyanate **17**.^[30] However, the extension to diamondoids in our case would necessitate to synthesize the corresponding organomagnesium derivatives and isocyanates, which would increase the complexity and hence likely decrease the overall yield. Due-Hansen et al. have shown, in 2015, that the coupling of the corresponding carboxylic acid **13** and amine **9** using fluoronium agents such as BTFFH (bis(tetramethylene)fluoroformamidinium hexafluorophosphate) provided **11a** in 78% yield.^[31] Finally, in the same year, Gallego-Yerga et al. synthesized **11a** by acylation of the amine hydrochloride **9·HCl** with the corresponding carbonyl chloride **12** in the presence of DIPEA with a yield of 87%.^[32] Keeping in mind that we aimed at using protocols that can be safely transposed to the more sterically hindered diamantane and azaadamantane moieties, and with the aim to use a procedure needing preferably no added (potentially expensive) reagents, we set aside the protocols using $[\text{BMIM}(\text{SO}_3\text{H})][\text{OTf}]$, fluoronium agent BTFFH and isocyanates or Grignard reagents. It is also worth noting that there are some examples of syntheses of amines or amides bearing adamantane fragments located further apart from each other, as in the previously described works of Kas'yan, Gallego-Yerga et al.^[27,32] However, the design of our desired compounds needs to meet a few criteria for good suitability towards the formation of fluorescent nanodiamonds, which are not met in these cited references. Indeed, according to our work hypotheses, the target molecules need to exhibit a close proximity between each diamondoid fragments, as well as having the nitrogen atom as close as possible to one of the fragments, and finally to avoid a high nitrogen content. These will be useful for limiting molecular displacement, good nitrogen incorporation in the diamond unit cell, and avoiding excessive nitrogen content in the diamond (since nitrogen-vacancy centers are usually present in ppm concentration). Since there are no published studies (at this time) dedicated to investigating the effect of the design of nitrogen-containing diamondoid precursors on nanodiamond formation, our target compounds will help confirm or refute these hypotheses. To the best of our knowledge, there has been no report on the linking of adamantane to diamantane and azaadamantane fragments meeting these criteria, which motivated us to further investigate this synthetic transformation and to extend the synthetic toolbox of diamondoid functionalization chemistry.

Results and Discussion

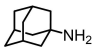
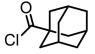
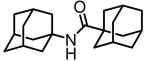
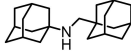
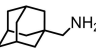
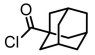
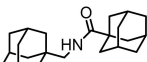
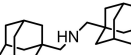
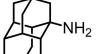
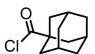
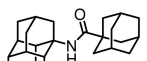
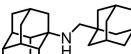

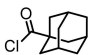


Synthesis

The first investigations were carried out by following the procedure of Dubowchik et al. for the formation of **11a**.^[21] The reaction mixture was gel-like in these conditions and led to the formation of mixtures of compounds among which the desired amide was identified. Further attempts at identifying the side products were unfruitful. Since we were looking for a protocol that would be more straightforward and would not need additional purification steps such as chromatographic separation, we thereupon explored the procedure of Rudkevich et al.^[28] This protocol was indeed meeting these criteria since the amide **11a** could be isolated in 85% yield without any extensive purification. The same protocol was then applied to 1-adamantylmethylamine **18**, to 1-aminodiamantane **19** and to 2-azaadamantane **5** with similar success and without the need for chromatographic purification (63 to 93% yields of **20a–22a** were obtained, see Table 2). A noteworthy comment is that this procedure did not suffer from the higher steric demand of the amine fragments and did not require any heating or prolonged reaction time. All the obtained amides **11a** and **20a–22a** could then be reduced by the borane-THF complex, followed by methanolysis, providing the corresponding amines **11b** and **20b–22b** in yields of 83–95%. We note that lower (yet relatively good) yields were obtained in some cases on smaller scales (e.g., for **11a** and **11b**, see footnotes of Table 2). Nevertheless, the combined steps of amidation and reduction are straightforward, are not affected by higher steric demand, do not require any chromatographic purification and provide the desired amines in good yields (55–88% combined yield). We then attempted to further increase the adamantane content by submitting amines **11b** and **20b** to the same amidation conditions. However, both amines were unreactive under these conditions, even with increased reaction times (2 to 48 h) and temperatures (r.t. to 100°C), presumably due to the considerable steric demand compared to the starting amines. Even treatment of the less sterically-demanding amine **20b** under the conditions of Dubowchik et al. was ineffective with respect to further amidation of the compound.

Crystal Structure

Studying the way molecules are arranged relative to each other might shine light on the behavior of the compounds during the transformation into nanodiamonds. Additionally, knowing that diamondoids are bulky and rigid fragments, one could expect to observe sterically-induced structural features such as lengthened bonds or widened angles in the molecular structure, as we have also recently demonstrated with methylated bis-adamantyls.^[33,34] Therefore, we desired to elucidate the crystal structure of the amides and amines by single-crystal X-ray diffraction. Unfortunately, we were only able to obtain and solve the crystal structure of compounds **21b** and **22a**. The other compounds could either not be obtained as single

Table 2. Syntheses of amides 11 a and 20 a–22 a and amines 11 b and 20 b–22 b.^[a]

R ₁ fragment	R ₂ fragment	Product	Yield [%]	Reduction product	Reduction yield [%]
			85 ^[b]		92 ^[c]
			63		88
			79 ^[d]		83
			93 ^[e]		95

[a] Reagents and conditions: 1) amine (1.0 equiv.), carbonyl chloride (1.0 equiv.), K₂CO₃ (2.0 equiv.), EtOAc/H₂O (1 : 1), r. t., 2 h; 2) Amide (1.0 equiv.), BH₃·THF (1 M in THF, 2.0 equiv.), THF, 66 °C, 15 h; 3) MeOH, 65 °C, 45 min. [b] 74% on a 1 mmol scale. [c] 62% on a 0.6 mmol scale. [d] 75% on a 1.2 mmol scale. [e] 92% on a 0.7 mmol scale.

crystals (compounds **11 b**, **20 b** and **21 a**), or the solution to the X-ray diffraction gave disordered structures and hence unreliable/uninformative geometric parameters (compounds **11 a**, **20 a** and **22 b**).

The structural features of **21 b** and **22 a** were compared with diamondoid amines and amides whose crystal structures had been solved and reported, and with reference to tabulated bond lengths.^[35] The CCDC and IUCr depositories contain a few entries for amides derived from adamantane. Entries were selected based on two criteria: a diamondoid moiety must be a direct substituent either on the N-side or on the acyl side, and the other substituents must either be a hydrogen or an alkyl chain (to avoid inductive or conjugative effects). Three entries with an adamantane moiety on the N-side were found, and only one entry with an adamantane moiety on the acyl side was found.^[36–39] For **22 a**, the N–C(=O) bond length amounts to 1.3642(16) Å, which is longer than typical tertiary amide N–C(=O) bonds of 1.346 Å and longer than the bond lengths found in the deposited structures, which feature N–C(=O) bond lengths of 1.333–1.345 Å (see Figure 2). The C(=O)–C bond is also longer, with a bond length of 1.5478(17) Å compared to a typical tabulated value of 1.533 Å and 1.501–1.527 Å for the deposited structures. These observations have their origins in the exacerbated rigidity and bulkiness of **22 a** compared to typical amides and even other adamantane-derived amides. Additionally, the C=O bond is 16.0° out-of-plane below the azaadamantane CNC plane. The carbonyl carbon and oxygen atoms lie 0.242 and 0.577 Å below this plane, respectively. This is due to the steric interaction between C=O and (*cis*)-α(C–H), since the conformation of (*cis*)-α(C–H) is locked by the rigid azaadamantane core. Data comparison with the deposited structures further confirms this out-of-average structural feature since the out-of-planarity is usually low (between 1 and 4°) and the distance with the plane is typically lower than 0.1 Å (i.e., they can

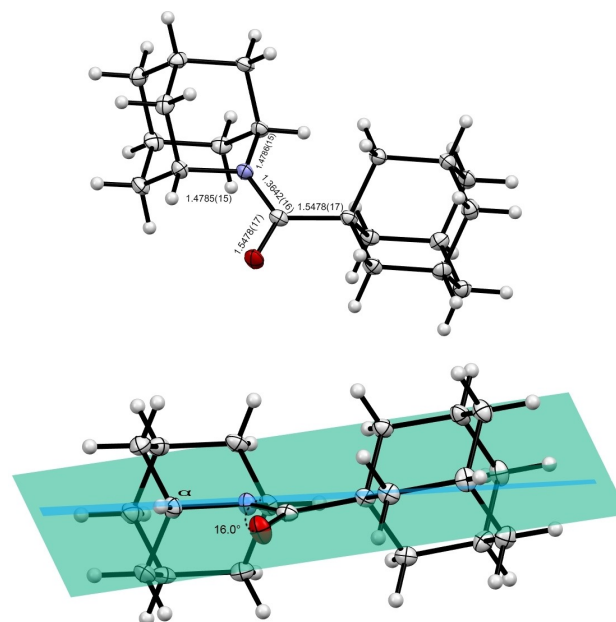


Figure 2. ORTEP diagrams of compound **22 a** with displacement ellipsoids drawn at the 50% probability level (grey: carbon, blue: nitrogen, red: oxygen, white: hydrogen). Bond lengths are given in Å.

confidently be considered in-plane in these cases). Amide **22 a** is therefore different from other amides derived from adamantane and exhibits structural features that are uncommon compared to most other amides. For completeness, there are other examples of very twisted amides derived from 1-azaadamantane.^[40,41] However, they differ from **22 a** since the carbonyl group is located directly on the core and its conformation is locked. No significant influence of crystal packing on the molecular geometries of **22 a** are expected since all intermolecular close-contact distances lie in the typically expected ranges of around 2.2–2.5 Å.^[42,43] Given the

exceptional out-of-planarity of the C=O bond in **22a**, one could expect that, if the contribution of crystal packing on the molecular geometry was significant, intermolecular close contacts would differ from average values. Since this is not the case, crystal packing only has a limited effect on the exceptional structural features of **22a**. Compound **21b**, on the other hand, does not feature any exceptionally elongated bonds, deviations from (non)planarity or widened angles and therefore can be considered as a typical amine, even if the substituents are rather bulky (see Figure 3).

NMR Studies

During the NMR-spectroscopic characterization of compound **22a**, we observed only one ^1H signal for the CH protons in α position to the nitrogen atom. Given that *N,N*-dimethylformamide and other alkyl-substituted amides typically exhibit two sets of ^1H signals due to rotational exchange at room temperature, we expected to observe similar behavior. Additionally, **22a** exhibited a broad ^{13}C signal for CH_2 in β position, and an apparent lack of a ^{13}C signal for α carbons using CDCl_3 as the solvent. This was further clarified by changing solvents (benzene- d_6 or toluene- d_8), which resulted in a slight narrowing of the ^{13}C signal for carbons in β position and the observation of a very broad ^{13}C signal corresponding to carbons α . These observations are due to the rotational exchange from the hindered rotation around the amide bond. We therefore explored this phenomenon by dynamic NMR experiments (DNMR) in order to characterize the exchange mechanism. Samples of **22a** were analyzed by ^1H and ^{13}C NMR spectroscopy in CDCl_3 , tetrachloroethane- d_2 (TCE- d_2) and toluene- d_8 at temperatures ranging from -50°C to $+120^\circ\text{C}$, depending on the solvent. The reason for using different solvents was twofold: first, to extend the available temperatures that can be explored (the boiling point of CDCl_3 is 60°C , while for TCE- d_2 , this value is 147°C), and second, to compare the effect of solvent polarity. As can be seen in the experimental ^1H NMR spectra in Figure 4, there is evidence of an exchange mechanism. Indeed, protons α have two different resonance frequencies at low temperatures

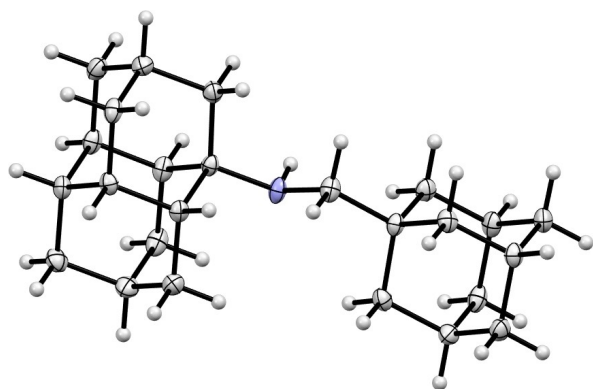


Figure 3. ORTEP diagram of compound **21b** with displacement ellipsoids drawn at the 50% probability level (grey: carbon, blue: nitrogen, white: hydrogen). Bond lengths are given in Å.

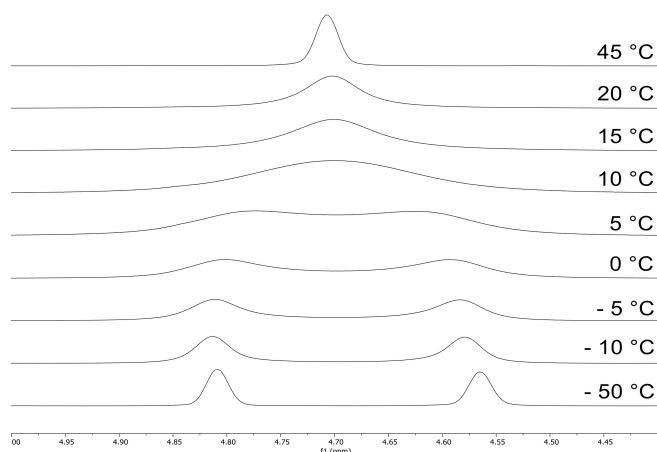


Figure 4. Selection of representative ^1H NMR spectra of **22a** in CDCl_3 at various temperatures at 400 MHz. The zoomed-in section corresponds to CH in α positions. The intensity scale is independently modified for representation purposes.

(due to inequivalence) and one unique resonance frequency at higher temperatures (due to fast interconversion). No other sets of protons exhibited any exchange phenomenon on this time-scale in the studied solvents and temperatures ranges (in particular protons β which are the second-closest protons to the nitrogen). At constant temperature, no significant change in pattern or position of the signals of **22a** in low or high concentration was observed. Activation parameters were determined according to the commonly used approximation method of Gasparro and Kolodny and are presented in Table 3.^[44] (Complete description of the calculations methods, as well as Eyring plots and complete stacks of ^1H NMR spectra at various temperatures are presented in the Supporting Information.)

In all three cases, the entropy component is small, as is typically the case for conformational exchanges and the process is therefore mostly enthalpy-driven.^[45,46] The calculated rotational free energies of activation are similar when calculated either using the modified Eyring equation or $\Delta G^\ddagger = \Delta H^\ddagger - T_c \Delta S^\ddagger$ which gives confidence in the calculated values of ΔH^\ddagger and ΔS^\ddagger from the Eyring plot. It is worth noting that the high relative errors of ΔS^\ddagger are to be put into perspective with the

Table 3. Selected calculated thermodynamic parameters for the amide bond rotation of **22a**.^[a]

Parameter	CDCl_3	TCE- d_2	Toluene- d_8
T_c (K)	280	283	261
k_c (s^{-1})	216	180	650
ΔH^\ddagger ^[b] ($\text{kcal} \cdot \text{mol}^{-1}$)	12.4 ± 0.4	12.0 ± 0.3	11.5 ± 0.3
ΔS^\ddagger ^[b] ($\text{cal} \cdot \text{mol}^{-1} \cdot \text{K}^{-1}$)	-2.1 ± 1.4	-4.3 ± 1.0	0.3 ± 1.2
ΔG^\ddagger ^[c] ($\text{kcal} \cdot \text{mol}^{-1}$) at T_c	13.0	13.2	11.5
ΔG^\ddagger ^[d] ($\text{kcal} \cdot \text{mol}^{-1}$) at T_c	13.0 ± 0.8	13.2 ± 0.6	11.5 ± 0.6
ΔG^\ddagger ^[d] ($\text{kcal} \cdot \text{mol}^{-1}$) at 298 K	13.0 ± 0.8	13.3 ± 0.6	11.5 ± 0.6

[a] Detailed explanations on the calculations are presented in the Supporting Information; [b] calculated from Eyring plots; [c] calculated from the modified Eyring equation; [d] calculated from the relation $\Delta G^\ddagger = \Delta H^\ddagger - T \Delta S^\ddagger$.

near-zero value of the entropy component.^[46,47] There is a decrease of activation free energy of rotation from CDCl_3 or $\text{TCE-}d_2$ to toluene- d_6 . This behavior originates from the difference of polarity of the solvents. It has previously been postulated that rotation around an amide bond proceeds via two transition states with pyramidalization at the nitrogen and that these transition states have lower dipole moments than the ground state.^[48–50] Consequently, polar solvents stabilize the ground state to a greater extent, resulting in a higher activation free energy of rotation. Because toluene- d_6 has a lower polarity than CDCl_3 and $\text{TCE-}d_2$, the energy of activation in this solvent is lower, which is the observed result. Additionally, the ΔG^\ddagger values in all three solvents (11–13 $\text{kcal}\cdot\text{mol}^{-1}$) are significantly lower than for most amides, which are typically in the 15–20 $\text{kcal}\cdot\text{mol}^{-1}$ range.^[51,52] This is due to the size of the azaadamantane and adamantane substituents. Indeed, it has previously been shown that an increase in the size of the substituents on the nitrogen and on the acyl sides results in a lower activation free energy of rotation. This is rationalized in terms of the increase in repulsive interactions in the planar ground state compared to the pyramidalized transition states, which consequently reduces the energy barrier, as evidenced by calculations and computational methods.^[51,53–56] This is further exacerbated by the distortion of the amide linkage at the ground state on increasing the steric effects of the substituents.^[54–56] For examples, the rotational activation barrier of *N,N*-dimethylformamide $\text{HC}(=\text{O})\text{N}(\text{CH}_3)_2$ is around 20–21 $\text{kcal}\cdot\text{mol}^{-1}$,^[49,57] the value for *N,N*-dimethylacetamide $\text{H}_3\text{CC}(=\text{O})\text{N}(\text{CH}_3)_2$ is around 17–18 $\text{kcal}\cdot\text{mol}^{-1}$,^[49,57,58] and for *N,N*-dimethylpivalamide $(\text{CH}_3)_3\text{CC}(=\text{O})\text{N}(\text{CH}_3)_2$, the value is around 11–12 $\text{kcal}\cdot\text{mol}^{-1}$.^[49,52] As a comparison, our experimental values for **22a** are close to the values of *N,N*-dimethylpivalamide and seem to be the lowest limit of activation free energy of rotation in alkyl-substituted amides. Even though this exchange phenomenon is related to the properties in solution, we speculate that it can also provide valuable insights into the effect of conformational exchanges to solid-state transformation of molecular precursors in high-pressure high-temperature conditions. Indeed, the influence of hindered rotation or motion is still unknown regarding the conversion into nanodiamonds, which is an effect that we are interested in studying further in the future. Fast and slow exchange mechanisms were also observed in the ^{13}C spectra for carbons α and β in all three solvents. This further confirms the broad ^{13}C NMR signal that was observed for CH_2 in β position, and the apparent lack of a ^{13}C NMR signal for α carbons in CDCl_3 at room temperature. A more complete study of the rotational exchange based on the ^{13}C NMR spectra was not performed since the exchange could be studied from the ^1H NMR spectra, and because a reliable determination of the activation parameters from ^{13}C NMR spectra is more difficult to obtain. (^{13}C NMR spectra for these signals at various temperatures are presented in the Supporting Information.) None of the other obtained amides and amines exhibited a similar exchange behavior in the ^1H or ^{13}C NMR spectra (either at room temperature or at -50°C in CDCl_3 and toluene- d_6) despite the enhanced steric strain of the diamondoid moieties. One could have expected that, for example,

compound **21a** would have shown hindered rotation around the amide bond due to the bulkiness of the diamantane fragment, despite the fact that it is a secondary amide. Notwithstanding the generally low-energy barrier of rotation in amines ($< 6 \text{ kcal}\cdot\text{mol}^{-1}$), one could have expected to observe a hindered rotation due to bulkiness.^[53] Additional studies at even lower temperatures ($< -50^\circ\text{C}$) might further slow down the exchange; however, we consider this out of the frame of our studies as it represents an extreme behavior of limited interest in our case.

Thermal Properties

The thermal behavior of the compounds is an important factor towards assessing the suitability of the molecules for the formation of fluorescent nanodiamonds. Indeed, degradation of the compounds might indicate that the molecule would not survive the HPHT conditions and would not have an influence on the transformation to nanodiamonds. The thermal behavior of the obtained amides **11a** and **20–22a** and of amines **11b** and **20–22b** was thus studied by melting point determination and thermogravimetric analyses (TGA). The latter would be particularly indicative of any degradation or thermally-induced transformation. Upon measurement of melting points, all the compounds exhibited immediate vaporization after melting. Thermogravimetric analyses under nitrogen atmosphere revealed that all the compounds are subliming or vaporizing at temperatures in the 200–300 $^\circ\text{C}$ range with complete mass loss (see Figure 5). ^1H NMR analyses of the recovered vaporized samples indicated no structural changes or degradation for all compounds. Therefore, they are all stable in the studied temperature range. As expected, the amides are subliming or vaporizing at higher temperatures than their corresponding amines due to increased hydrogen bonding (or, more broadly, increased intermolecular interactions, since compound **22a** does not exhibit hydrogen bonding). This can be seen from the higher temperature values of the onset temperatures in TGA curves and of DTG (derivative thermogravimetry) peak temperatures for the amides, summarized in Table 4. Interestingly, the temperature increase from amine to amide is similar for the class of compounds **11a–b** and **20a–b** (increase of 28–31 $^\circ\text{C}$), which are the most structurally alike molecules of the set. Comparatively, the temperature increase for **22a–b** is higher (39–44 $^\circ\text{C}$), and minimal for **21a–b** (8–15 $^\circ\text{C}$). Another observation is that the onset temperature and peak DTG temperatures are rising with increased molecular weight among the amines and amides series (see Figure 5). This is representative of the expected raise of dispersion forces. These observations are to be compared with the obtained melting point values. Except for **22a**, which does not exhibit hydrogen bonding, melting points are inversely correlated to molecular weight. This can be attributed to the different phase changes that are studied during melting point determination experiments and TGA experiments. Indeed, while the melting point temperatures are characteristic of solid-to-liquid phase transitions, TGA onset and DTG peak temperatures are representative of liquid-to-gas

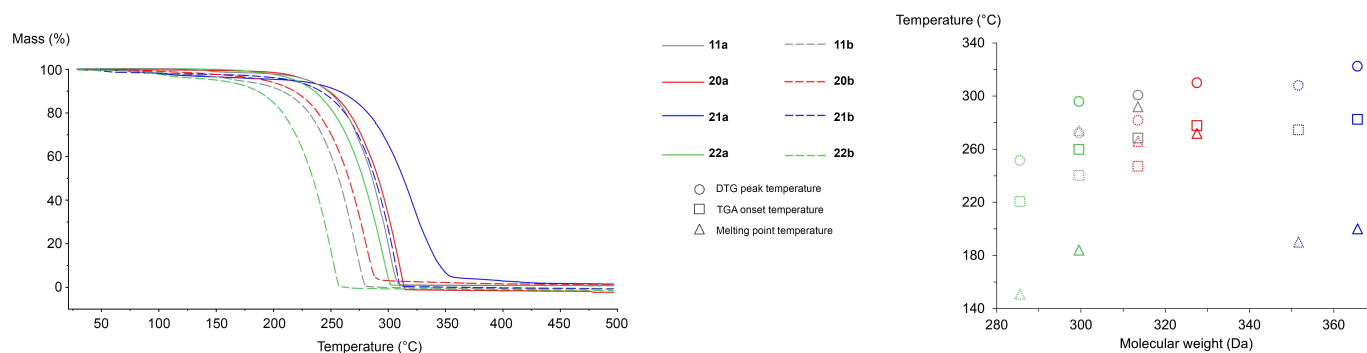


Figure 5. TGA curves and thermal properties of compounds 11 a–b, 20 a–b, 21 a–b and 22 a–b.

Table 4. Thermal properties of compounds 11 a–b, 20 a–b, 21 a–b and 22 a–b. ^[a]							
Compound	Molecular weight [Da]	Onset temperature [°C]	DTG peak temperature [°C]	DTG peak temperature [°C]	DTG peak temperature [°C]	DTG peak temperature [°C]	DTG peak temperature [°C]
11 a	313.5	268	301	292			
11 b	299.5	240	272	274			
		$\Delta T_{11a-11b} = 28$		$\Delta T_{11a-11b} = 29$			$\Delta T_{11a-11b} = 18$
20 a	327.5	278	310	272			
20 b	313.5	247	282	266			
		$\Delta T_{20a-20b} = 31$		$\Delta T_{20a-20b} = 28$			$\Delta T_{20a-20b} = 6$
21 a	365.6	283	323	199–202			
21 b	351.6	275	308	190–191			
		$\Delta T_{21a-21b} = 8$		$\Delta T_{21a-21b} = 15$			$\Delta T_{21a-21b} = 8-12$
22 a	299.5	260	296	183–185			
22 b	285.5	221	252	150–152			
		$\Delta T_{22a-22b} = 39$		$\Delta T_{22a-22b} = 44$			$\Delta T_{22a-22b} = 31-35$

[a] TGA experiments were performed at 10 °C min⁻¹ under a nitrogen atmosphere.

phase transitions because they are typically superior to the melting point temperatures in these cases. Therefore, the experimental values described here for melting points are illustrative of solid-state properties, while the values for TGA and DTG are indicative of liquid-state properties. Additionally, melting point temperatures are dependent on multiple factors such as packing, polymorphism, and the amorphous or crystalline nature of the solid, which do not have an influence on the liquid-phase properties. We suggest that the inverse correlation between melting points and molecular weight (except for **22 a**) is due to the spatial redistribution of hydrogen bonding in the solid due to the increase of space taken by the molecules in the solid. Therefore, the hydrogen bonding interactions are decreased and the melting point is lowered. Nonetheless, this would need a more definite rationalization based on additional data on a much larger study that would examine the thermal properties of amides and amines (in the broad sense, not limited to diamondoids) at the solid-liquid state transition. This is, however, out of the scope of the current manuscript.

Conclusion

Amides and amines containing two adamantane, azaadamantane or diamantane fragments were synthesized in good yields. This protocol is compatible with sterically-demanding diamond-

oid fragments and can be performed in a straightforward and easy way. The crystal structure of the most crowded amide **22 a** revealed exceptional structural features such as elongated bonds and deviations from planarity of the amide C=O bond due to steric congestion. Furthermore, the activation parameters of amide bond rotation of **22 a** were determined by dynamic NMR experiments and the obtained low rotational free energy of the amide bond was in agreement with the pyramidalization mechanism of amide rotation and is explained by the steric congestion of the substituents. Results of thermal analyses indicated that all compounds are resilient to degradation in the studied temperature range. All these structural and material characterizations are valuable piece of information for the future use of these compounds for the formation of fluorescent nanodiamonds.

Experimental Section

General Procedure A: Formation of Amides 11 a and 20–22 a

To a round-bottom flask were added the amine (1.0 equiv.) and K₂CO₃ (2.0 equiv.) in EtOAc/H₂O (1:1, 10 mL per mmol of amine). Then, 1-adamantanecarbonyl chloride (1.0 equiv.) was added as a solid in one portion under vigorous stirring at room temperature. The reaction mixture was then stirred vigorously for 2 h. The reaction mixture and the formed solid were then either filtered on a fritted glass and washed with distilled H₂O (the collected solid

being the desired amide), or CH_2Cl_2 was added to the organic phase, which was then washed with distilled H_2O and brine. The organic phase was then dried over MgSO_4 , filtered and concentrated under reduced pressure, allowing the isolation of the desired amide as a white solid.

General Procedure B: Formation of Amines 11 b and 20–22 b

To a round-bottom flask was added the amide (1.0 equiv.) in anhydrous THF (4 mL per mmol of amide) under argon at 0°C . Then, borane-THF complex was added (1 M in THF, 2.0 equiv.) and the solution was stirred overnight at 66°C . The reaction was cooled down to 0°C and quenched by the dropwise addition of MeOH. The solvents were evaporated under reduced pressure and excess MeOH (10 mL per mmol of starting material) was added to the obtained white solid. The reaction mixture was stirred 45 minutes at 65°C . The solvent was evaporated, and CH_2Cl_2 was added to the white crude solid. The mixture was then washed with distilled H_2O and brine. The organic phase was then dried over MgSO_4 , filtered and concentrated under reduced pressure, allowing the isolation of the amine as a white solid.

Full Supporting Information available: Detailed experimental procedures, characterization data, ^1H and ^{13}C NMR and VT NMR spectra, Eyring plots, TGA and DTG measurements, X-ray structures and crystallographic data. Deposition Numbers 2121891 (for 21 b) and 2121892 (for 22 a) contain the supplementary crystallographic data for this paper. These data are provided free of charge by the joint Cambridge Crystallographic Data Centre and Fachinformationszentrum Karlsruhe Access Structures service.

Acknowledgements

This work was supported by the Fonds de la Recherche Scientifique – FNRS under Grants Pi-Fast n° T.0072.18, and 2Dto3D n° 30489208. Y. G. also acknowledges financial supports from the French Community of Belgium (ARC n° 20061). M. B. is a Research Fellow of the Fonds de la Recherche Scientifique – FNRS.

Conflict of Interest

The authors declare no conflict of interest.

Data Availability Statement

The data that support the findings of this study are available in the supplementary material of this article.

Keywords: adamantane · amide formation · bond rotation · cage compounds · steric strain

- [1] L. Wanka, K. Iqbal, P. R. Schreiner, *Chem. Rev.* **2013**, *113*, 3516–3604.
- [2] K. Spilovska, F. Zemek, J. Korabecny, E. Nepovimova, O. Soukup, M. Windisch, K. Kuca, *Curr. Med. Chem.* **2016**, *23*, 3245–3266, <https://doi.org/10.2174/0929867323666160525114026>.
- [3] E. A. Ekimov, K. M. Kondrina, N. E. Mordvinova, O. I. Lebedev, D. G. Pasternak, I. I. Vlasov, *Inorg. Mater.* **2019**, *55*, 437–442.

- [4] O. S. Kudryavtsev, E. A. Ekimov, A. M. Romshin, D. G. Pasternak, I. I. Vlasov, *Phys. Status Solidi A* **2018**, *215*, 1800252.
- [5] E. A. Ekimov, K. M. Kondrina, I. P. Zibrov, S. G. Lyapin, M. V. Lovygin, P. R. Kazanskiy, *Mater. Res. Bull.* **2021**, *137*, 111189.
- [6] J. Liang, C. P. Ender, T. Zapata, A. Ermakova, M. Wagner, T. Weil, *Diamond Relat. Mater.* **2020**, *108*, 108000.
- [7] E. A. Ekimov, O. S. Kudryavtsev, N. E. Mordvinova, O. I. Lebedev, I. I. Vlasov, *ChemNanoMat* **2018**, *4*, 269–273.
- [8] E. A. Ekimov, S. G. Lyapin, Yu. V. Grigoriev, I. P. Zibrov, K. M. Kondrina, *Carbon* **2019**, *150*, 436–438.
- [9] E. A. Ekimov, M. V. Kondrin, S. G. Lyapin, Yu. V. Grigoriev, A. A. Razgulov, V. S. Krivobok, S. Gierlotka, S. Stelmakh, *Diamond Relat. Mater.* **2020**, *103*, 107718.
- [10] E. A. Ekimov, S. G. Lyapin, Yu. V. Grigor'ev, *Inorg. Mater.* **2020**, *56*, 338–345.
- [11] M. Alkahtani, J. Lang, B. Naydenov, F. Jelezko, P. Hemmer, *ACS Photonics* **2019**, *6*, 1266–1271.
- [12] Y.-K. Tzeng, J. L. Zhang, H. Lu, H. Ishiwata, J. Dahl, R. M. K. Carlson, H. Yan, P. R. Schreiner, J. Vučković, Z.-X. Shen, N. Melosh, S. Chu, *Nano Lett.* **2017**, *17*, 1489–1495.
- [13] V. N. Mochalin, O. Shenderova, D. Ho, Y. Gogotsi, *Nat. Nanotechnol.* **2012**, *7*, 11–23.
- [14] J.-C. Arnault, *Nanodiamonds: Advanced Material Analysis, Properties and Applications*, Elsevier, Amsterdam, **2017**, <https://doi.org/10.1016/C2015-0-01721-X>.
- [15] M. D. Torelli, N. A. Nunn, O. A. Shenderova, *Small* **2019**, *15*, 1902151.
- [16] M. H. Alkahtani, F. Alghannam, L. Jiang, A. Almethen, A. A. Rampersaud, R. Brick, C. L. Gomes, M. O. Scully, P. R. Hemmer, *Nanophotonics* **2018**, *7*, 1423–1453, <https://doi.org/10.1515/nanoph-2018-0025>.
- [17] G. Balasubramanian, A. Lazariev, S. R. Arumugam, D. Duan, *Curr. Opin. Chem. Biol.* **2014**, *20*, 69–77.
- [18] I. K. Moiseev, N. V. Makarova, M. N. Zemtsova, *Russ. Chem. Rev.* **1999**, *68*, 1001–1020.
- [19] M. A. Gunawan, J.-C. Hierro, D. Poinot, A. A. Fokin, N. A. Fokina, B. A. Tkachenko, P. R. Schreiner, *New J. Chem.* **2014**, *38*, 28–41.
- [20] E. V. Krumkalns, W. Pfeifer, *J. Med. Chem.* **1968**, *11*, 1103.
- [21] G. M. Dubowchik, L. Padilla, K. Edinger, R. A. Firestone, *J. Org. Chem.* **1996**, *61*, 4676–4684.
- [22] H. Sarker, M. L. Greer, S. C. Blackstock, *J. Org. Chem.* **1996**, *61*, 3177–3182.
- [23] C. E. Wagner, M. L. Mohler, G. S. Kang, D. D. Miller, E. E. Geisert, Y.-A. Chang, E. B. Fleischer, K. J. Shea, *J. Med. Chem.* **2003**, *46*, 2823–2833.
- [24] A. Debuigne, D. Chan-Seng, L. Li, G. K. Hamer, M. K. Georges, *Macromolecules* **2007**, *40*, 6224–6232.
- [25] M. Mesgar, J. Nguyen-Le, O. Daugulis, *J. Am. Chem. Soc.* **2018**, *140*, 13703–13710.
- [26] M. Mesgar, J. Nguyen-Le, O. Daugulis, *Chem. Commun.* **2019**, *55*, 9467–9470.
- [27] L. I. Kas'yan, D. V. Karpenko, A. O. Kas'yan, A. K. Isaev, S. A. Prid'ma, *Russ. J. Org. Chem.* **2007**, *43*, 1642–1650, <https://doi.org/10.1134/S1070428007110103>.
- [28] D. M. Rudkevich, G. Hilmersson, J. Rebek, *J. Am. Chem. Soc.* **1998**, *120*, 12216–12225.
- [29] R. G. Kalkhambkar, S. N. Waters, K. K. Laali, *Tetrahedron Lett.* **2011**, *52*, 867–871.
- [30] G. Schäfer, C. Matthey, J. W. Bode, *Angew. Chem. Int. Ed.* **2012**, *51*, 9173–9175; *Angew. Chem.* **2012**, *124*, 9307–9310.
- [31] M. E. Due-Hansen, S. K. Pandey, E. Christiansen, R. Andersen, S. V. F. Hansen, T. Ulven, *Org. Biomol. Chem.* **2015**, *14*, 430–433, <https://doi.org/10.1039/C5OB02129D>.
- [32] L. Gallego-Yerga, L. Blanco-Fernández, K. Urbiola, T. Carmona, G. Marcelo, J. M. Benito, F. Mendicuti, C. Tros de Ilduya, C. Ortiz Mellet, J. M. García Fernández, *Chem. Eur. J.* **2015**, *21*, 12093–12104, <https://doi.org/10.1002/chem.201501678>.
- [33] P. R. Schreiner, L. V. Chernish, P. A. Gunchenko, E. Y. Tikhonchuk, H. Hausmann, M. Serafin, S. Schlecht, J. E. P. Dahl, R. M. K. Carlson, A. A. Fokin, *Nature* **2011**, *477*, 308–311.
- [34] M. Bonsir, C. Davila, A. R. Kennedy, Y. Geerts, *Eur. J. Org. Chem.* **2021**, *2021*, 5227–5237, <https://doi.org/10.1002/ejoc.202101004>.
- [35] F. H. Allen, O. Kennard, D. G. Watson, L. Brammer, A. G. Orpen, R. Taylor, *J. Chem. Soc. Perkin Trans. 2* **1987**, 51–519, <https://doi.org/10.1039/P29870000051>.
- [36] A. E. Prozorovskii, V. A. Tafeenko, V. B. Rybakov, É. A. Shokova, V. V. Kovalev, *J. Struct. Chem.* **1987**, *28*, 243–251.

- [37] H.-H. Pröhl, A. Blaschette, P. G. Jones, *Acta Crystallogr. Sect. C* **1997**, *53*, 1434–1436.
- [38] Y.-N. Yin, R.-Q. Ding, D.-C. Ouyang, Q. Zhang, R. Zhu, *Nat. Commun.* **2021**, *12*, 2552, <https://doi.org/10.1038/s41467-021-22373-z>.
- [39] W. Sima, *Acta Crystallogr. E Struct. Rep. Online* **2009**, *65*, o2492–o2492.
- [40] A. J. Kirby, I. V. Komarov, P. D. Wothers, N. Feeder, *Angew. Chem. Int. Ed. Engl.* **1998**, *37*, 785–786.
- [41] I. V. Komarov, S. Yanik, A. Yu. Ishchenko, J. E. Davies, J. M. Goodman, A. J. Kirby, *J. Am. Chem. Soc.* **2015**, *137*, 926–930.
- [42] J. D. Dunitz, A. Gavezzotti, *Acc. Chem. Res.* **1999**, *32*, 677–684.
- [43] S. Alvarez, *Dalton Trans.* **2013**, *42*, 8617–8636.
- [44] F. P. Gasparro, N. H. Kolodny, *J. Chem. Educ.* **1977**, *54*, 258.
- [45] C. Piccinni-Leopardi, O. Fabre, J. Reisse, *Org. Magn. Reson.* **1976**, *8*, 233–236.
- [46] D. Casarini, L. Lunazzi, A. Mazzanti, *Eur. J. Org. Chem.* **2010**, *2010*, 2035–2056, <https://doi.org/10.1002/ejoc.200901340>.
- [47] A. Allerhand, H. S. Gutowsky, J. Jonas, R. A. Meinzer, *J. Am. Chem. Soc.* **1966**, *88*, 3185–3194.
- [48] C. Cox, T. Lectka, *J. Org. Chem.* **1998**, *63*, 2426–2427.
- [49] T. Drakenberg, K. I. Dahlqvist, S. Forsen, *J. Phys. Chem.* **1972**, *76*, 2178–2183.
- [50] E. S. Eberhardt, S. N. Loh, A. P. Hinck, R. T. Raines, *J. Am. Chem. Soc.* **1992**, *114*, 5437–5439.
- [51] K. Umemoto, K. Ouchi, *Proc. Indian Acad. Sci. Chem. Sci.* **1985**, *94*, 1–119.
- [52] M. D. Wunderlich, L. K. Leung, J. A. Sandberg, K. D. Meyer, C. H. Yoder, *J. Am. Chem. Soc.* **1978**, *100*, 1500–1503.
- [53] H. Kessler, *Angew. Chem. Int. Ed. Engl.* **1970**, *9*, 219–235.
- [54] Y. Jean, I. Demachy, A. Lledos, F. Maseras, *J. Mol. Struct.* **2003**, *632*, 131–144.
- [55] G. N. Radael, R. M. Pontes, *Comput. Theor. Chem.* **2020**, *1187*, 112938.
- [56] J. I. Mujika, J. M. Matxain, L. A. Eriksson, X. Lopez, *Chem. Eur. J.* **2006**, *12*, 7215–7224.
- [57] K. B. Wiberg, P. R. Rablen, D. J. Rush, T. A. Keith, *J. Am. Chem. Soc.* **1995**, *117*, 4261–4270.
- [58] L. W. Reeves, R. C. Shaddick, K. N. Shaw, *Can. J. Chem.* **1971**, *49*, 3683–3691.

Manuscript received: February 8, 2022

Revised manuscript received: February 11, 2022